DESIGN AND EXPERIMENT OF SWEET POTATO COMBINE HARVESTER BASED ON TWO-SEGMENT POTATO SOIL SEPARATION DEVICE
/
基于两段式薯土分离装置甘薯联合收获机设计与试验

Ranbing YANG[1,2], Minsheng WU[1,2], Peng XU[3], Yongfei PAN[1,2], Danyang LV[1,2], Xiantao ZHA*[1,2]
[1] School of Mechanical and Electrical Engineering, Hainan University, Hainan/ China;
[2] Key Laboratory of Tropical Intelligent Agricultural Equipment, Ministry of Agriculture and Rural Affairs, Hainan/ China;
[3] College of Engineering, Jiangxi Agricultural University, Jiangxi/ China
Corresponding author: Xiantao Zha
Tel: +8618627838628; E-mail: zhaxt@hainanu.edu.cn
DOI: https://doi.org/10.35633/inmateh-74-45

Keywords: *agricultural machinery, sweet potato, two-segment potato-soil separation, low damage harvesting, field experiment*

ABSTRACT
Aiming at the problems of high skin-breaking rate and high impurity rate of sweet potato during harvesting operations, a low-damage fresh-eating sweet potato combine harvester based on a two-segment potato-soil separation device was designed by using a "d"-type elevator chain combined with a double-buffer clearing platform technology. The results show that the best working parameters of the harvester are a vibrating shaft frequency of 5.2 Hz, elevator chain speed of 0.37 m/s, and cleaning platform speed of 0.58 m/s, in which the sweet potato skin-breaking rate is 1.09% and the impurity rate is 1.90%, which is in line with the standard.

摘要
针对甘薯收获作业过程中存在甘薯破皮率高、含杂率高的问题，采用"d 型升运链式薯土分离装置+双重缓冲清选平台"技术，设计了一种基于两段式薯土分离装置的低损鲜食甘薯联合收获机。结果表明，收获机最佳工作参数为振动轴频率 5.2Hz、升运链速度 0.37m/s、清选平台速度为 0.58m/s，此时甘薯破皮率为 1.09%、含杂率为 1.90%，符合标准。

INTRODUCTION
The sweet potato is characterized by a high and stable yield, drought resistance and barrenness tolerance, extensive adaptability, rich nutrition, etc. It occupies an important position in global agricultural production, and its market demand is increasing *(Bovell-Benjamin, 2007; dos Santos et al., 2019; Xie et al., 2022; Cláudio et al., 2020; Mohanraj et al., 2014)*. The current sweet potato harvesting method adopts a semi-mechanized operation mode, which causes the sweet potatoes to break during the potato soil separation process and mix with excessive soil, weeds and other impurities, seriously affecting the quality and market competitiveness of sweet potatoes *(Hu et al., 2014; Chen, 2020)*. In order to improve the performance of sweet potato harvesters, researchers conducted research from different angles. Hrushetsky and Fu developed an excavation device for potato harvesters, which significantly improved the excavation efficiency and reduced resistance, but had little impact on the peeling rate and potato soil separation rate *(Hrushetsky et al., 2019; Fu et al., 2023)*. The peeling rate and potato soil separation rate are the most important indicators for evaluating the performance of fresh sweet potato harvesters. Therefore, it is of great significance to develop high efficiency and low damage fresh sweet potato combine harvester, explore and optimize potato soil separation device, improve sweet potato harvest efficiency and reduce the rate of peeling and impurity.

In recent years, researchers have continuously innovated and optimized the structure of the potato-soil separator to improve its harvesting efficiency and sweet potato quality. For example, to reduce the skin-breaking rate of sweet potatoes, Marciniak, Cui, Ismail and Bulgakov developed a small-scale traction-type sweet potato harvester, and the developed machinery shortened the length of the potato-soil separating device, which resulted in less collision between sweet potatoes and rods and therefore a lower skin-breaking rate of

[1,2] *Ranbing Yang, Prof. Ph.D. Eng; Minsheng Wu, M.S. Stud. Eng; Yongfei Pan, Ph.D. Eng; Danyang Lv, Ph.D. Eng; Xiantao Zha, Ph.D. Eng.*
[3] *Peng Xu, Ph.D. Eng.*

sweet potatoes. However, the conveyor device has a compact structure and a short conveyor stroke, resulting in a poor soil-clearing effect and high subsequent labor intensity *(Marciniak et al., 2022; Cui et al., 2020; Ismail et al., 2014; Bulgakov et al., 2021; Feng et al., 2024)*. To improve the efficiency of potato-soil separation, researchers have increased the length and number of stages of the potato-soil separation device to reduce the impurity rate of sweet potatoes. For instance, Beznosyuk designed a multi-segment potato harvesting machine with transportation and clearing roles and mounted the multi-segment potato-soil separation device longitudinally to reduce the longitudinal clearance of sweet potatoes and the fall height during potato collection *(Beznosyuk et al., 2022)*. Li designed a ring-shaped damage-reducing potato collection and transportation device that uses a multi-stage transportation and cleaning method to clean the potato soil mixture of stones and vines, and the harvested potato crop is transported to the collection box *(Li et al., 2023)*. The above type of potato-soil separation device saves labor costs and has a high harvesting efficiency. The disadvantage is that, due to the excessively long potato-soil separation device, the number of collisions between sweet potatoes and the conveying device increases, resulting in an increased rate of skin breakage. In addition, due to the lack of manual cleaning, some stones and soil pieces are simple to transport into the collection box following the conveyor chain, which requires secondary cleaning *(Wei et al., 2023)*.

Combining the advantages and disadvantages of integrated and multi-segment potato-soil separation devices, some researchers have developed and designed a two-segment potato-soil separation device with a manual cleaning assistance platform. Yang created a new traction-type potato crop picking and bagging machine equipped with a two-segment flexible conveyor and a hydraulic control system, and they designed a rubberized bionic finger in the first segment of the elevator chain, which reduces the collision of the potato crop falling in the harvesting process (*Yang X. et al., 2024)*. Wang designed a self-propelled potato crop harvester for hilly and mountainous areas with a two-segment potato-soil separation device; the first segment of the potato-soil separation device is installed with a fingers-type crushing mechanism, and the second segment of the elevator chain is installed with a scraper to protect the sweet potatoes, which improves the harvesting efficiency and reduces the skin-breaking rate *(Wang et al., 2023)*. The two-segment potato-soil separation device improves the efficiency of potato-soil separation at the same time, supplemented by manual cleaning to minimize the impurity rate of sweet potatoes. However, there is still the problem of a high rate of broken skin in sweet potatoes, which still needs to be optimized by research and development personnel.

For the above problems, this paper develops and designs a two-segment potato-soil separation device that can complete the integration of the operations of sweet potato conveying, soil removal, cleaning, and collecting at one time, aiming at reducing the skin-breaking rate and impurity rate of sweet potato. The first segment of the "d" elevator chain potato-soil separation device realizes elevator chain straight bar sweet potato fall prevention, and the second segment of the double buffer cleaning platform realizes the optimization design of sweet potato fall damage. Field experiments were conducted using orthogonal testing to analyze and discuss the influence of each parameter on the skin-breaking rate and impurity rate, then to determine the optimal parameter combinations to improve the efficiency of sweet potato harvesting and to reduce the skin-breaking rate and impurity rate of sweet potatoes.

MATERIALS AND METHODS

Harvester structure and working principle

Combined with the agronomy of fresh-eating sweet potato cultivation in Hainan, China, a low-damage sweet potato combine harvester was designed based on a two-segment potato-soil separating device. The harvester consists of a profiling device, a digging device, a potato-soil separating device, a transmission system, a control console, and a traveling device, and its structure and object are shown in Figure 1.

In the sweet potato harvesting process, the harvester moves forward, and the profiling device carries out heaving motion according to the height of the ridge, realizing adaptive adjustment of digging depth. The digging shovel transports the potato-soil mixture to the first segment "d" type elevator chain potato-soil separation device, and a vibrating device is installed at the front end of the elevator chain to sieve off the redundant soil by vibrating it. The potato-soil mixture rotates with the elevator chain, passing through the drop buffer device to the second segment of the double buffer cleaning platform. The sweet potatoes are then cleaned by staff and placed on the inside of the potato collection board. The conveyor belt of the secondary double buffer cleaning platform carries the sweet potatoes to the rear conveying buffer device, and with the rotation of the rear conveying roller, it further cleans the soil adhering to the surface of the sweet potatoes. Finally, the sweet potatoes are decelerated by the rear rubber buffer curtain and fall into the potato collection basket to complete the harvesting process.

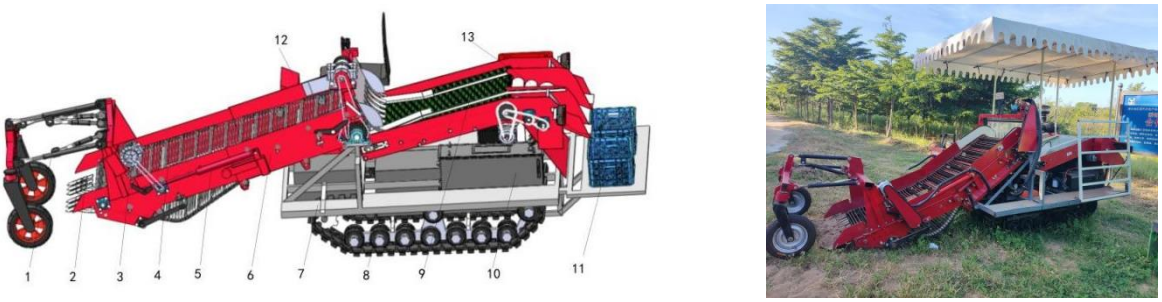

(a) (b)

Fig. 1 - Low-damage fresh sweet potato combine harvester

(a) Structure: 1 - profiling device; 2 - digging device; 3 - "d"-type elevator chain potato-soil separating device; 4 - hydraulic control device; 5 - frame; 6 - picking platform; 7 - crawler walking device; 8 - double buffer cleaning platform; 9 - fuel tank and power device; 10 - potato collection basket; 11 - control console; 12 - front falling buffer device; 13 - rear conveying buffer device. (b) Physical object

Transmission system and technical parameters

The transmission system of the low-loss fresh sweet potato combine harvester consists of hydraulic transmission and mechanical transmission, as shown in Figure 2. The engine transmits the power to the gearbox through the output shaft, which then transmits the power to the crawler-traveling device through the output shaft. The engine provides power for the hydraulic pump, and the change of the inclination angle of the elevator chain is controlled by the hydraulic pump's inlet and outlet oil volumes. The engine transmits the power to the vibrating shaft through the gearbox and the crank-rocker mechanism, which is used to separate the potato from the soil. The engine provides power for the "d" type elevator chain potato-soil separation device, double buffer cleaning platform, and conveying buffer device through the chain drive.

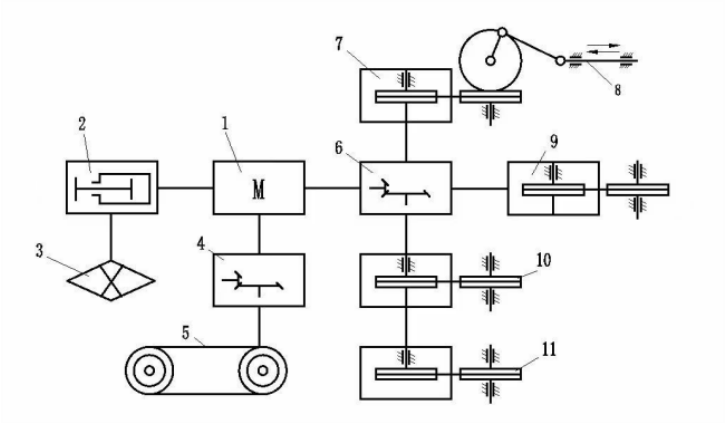

Fig. 2 - Schematic diagram of the transmission system of a low-damage fresh-eating sweet potato combine harvester

1 - engine; 2 - hydraulic pump; 3 - elevator chain inclination control; 4 - gearbox; 5 - crawler walking device; 6 - reducer; 7 - motor; 8 - vibrating shaft; 9 - elevator chain; 10 - conveyor belt; 11 - conveyor roller

Based on the harvesting demand of China's "Gaoxi 14" fresh sweet potato, the technical parameters of the low-damage fresh-eating sweet potato combine harvester are shown in Table 1.

Table 1

Technical parameters of low-damage fresh-eating sweet potato combine harvester

Parameters	Values
Structure form	Self-propelled
Power matching (HP)	70
Size (*L*×*W*×*H*)/(mm*mm*mm)	5500×2200×2000
Working width (mm)	1000
Digging depth (mm)	100-150 (below the bottom of the mound)
Operating speed (m/s)	0.2-0.7
Operating efficiency (m^2/h)	1400-2100
Potato collection method	Basket/Bagging
The whole machine's weight (kg)	2180

Design of one-segment "d" elevator chain potato-soil separation device

The compact structure of the traditional elevator chain and the use of tensioning devices limit the undulation and vibration of the elevator chain, which only ensures the vibration of the elevator chain on the vibrating shaft, with no extra space to support the vibration of the elevator chain in other positions. In addition, the clay loam and weeds carried by the traditional elevator chain are not cleaned in time, which makes it easy to increase its load and cause clogging of the chain plate and drive shaft *(Wang et al., 2014)*. For the above problems, this paper develops a first-segment "d" elevator chain potato-soil separation device, as shown in Figure 3. Near the digging shovel, the longer elevator chain is retained so that it falls under the action of the gravity of the rollers and the elevator chain itself, forming a structure similar to the letter "d". As shown in Figure 3 partial enlargement, the "d"-type elevator chain connecting belt is made of soft rubber material, conveying surface roller spacing between 30 and 50 cm between the rollers. Due to the elevator chain's self-gravity and potato-soil mixture quality, it is easy to cause the elevator chain to produce concave changes. Rollers can re-lift the elevator chain to achieve the conveying effect of gentle vibration and improve the efficiency of potato-soil separation. In the process of chain lifting, the excess elevator chain provides a force buffer for the conveying process. The falling part of the elevator chain can sieve the soil in time through the chain movement and the inertial swing of vehicle walking to reduce the redundancy of weeds and soil congestion at the front end of the elevator chain.

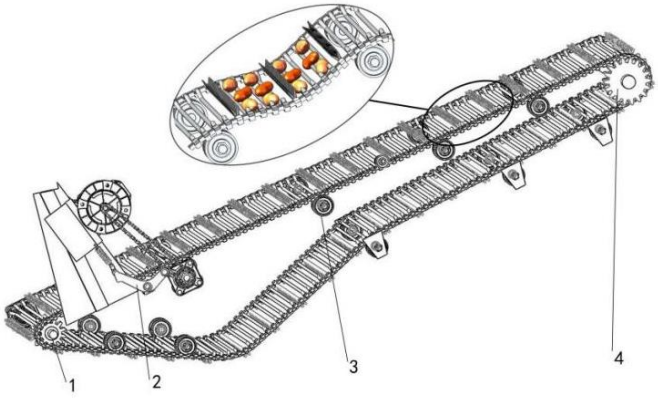

Fig. 3 - Structure of first-segment "d" elevator chain potato-soil separation device
1 - follower shaft; 2 - vibration device; 3 - rollers; 4 - active shaft

The elevator chain uses four continuous curved bars and one straight rubber bar. Nitrile rubber (NBR), a material that is small in hardness and has better adhesion to metal, forms both the rubber connecting belt and the rubber sleeve of the straight bar *(Shen, 2021)*. The straight bar's rubber sleeve shape is similar to the letter "V," which effectively protects the sweet potato when it rolls over in the elevator chain. Figure 4 illustrates the structural analysis of sweet potatoes in the elevator chain's curved bar zone.

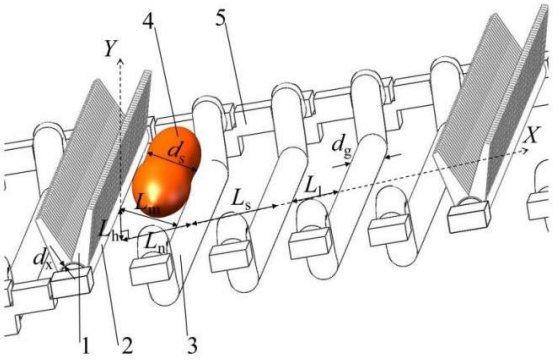

Fig. 4 - Sweet potatoes in the interval of the elevator chain curved bars
1 - rubber sleeve for the straight bar; 2 - straight bar; 3 - curved bar; 4 - sweet potato model; 5 - rubber connecting band.

It can be obtained from the analysis of Figure 4:

$$\begin{cases} L_s = L_l + d_g \\ L_h = \sqrt{\left(L_m + d_g + d_x\right)^2 - L_n{}^2} \end{cases} \quad (1)$$

where:

L_s is the centroid-distance between the curved rod and the curved bar on the X-axis, [mm]; L_n is the centroid-distance between the straight rod and the curved bar on the X-axis, [mm]; L_l is the gap between the curved rod and the curved bar, [mm]; d_g is the diameter of the bar, [mm]; L_h is the centroid-distance between the straight rod and the curved bar on the Y-axis, [mm]; L_m is the gap between the straight rod and the curved bar, [mm], and d_x is the thickness of the rubber sleeve wrapped around the straight rod bar, [mm].

In the current sweet potato harvester elevator chain structure, the bar diameter typically ranges from 9-11 mm *(Li et al., 2022)*. Combined with the actual operating conditions, a bar diameter d_g of 10 mm was selected. To reduce production costs and improve the elevator chain's stability, the distance between the links should be the same, i.e., L_n=L_s. To ensure optimal conveying performance, a large bar gap can enhance the efficiency of potato-soil separation. However, to decrease the loss of sweet potatoes, the bar gap should be smaller than the minimum short axis size. In the "agricultural machinery promotion appraisal outline" of potato harvester operation standard, the DG/T078-2022 establishes a minimum size of 25 mm for the sweet potato harvest loss rate *(Ministry of Agriculture and Rural Affairs, 2022)*. As a result, the gap between the straight bar and the curved bar, L_m, was set at 24 mm. The rubber sleeve thickness d_x, wrapped in the straight bar, d_x is 2 mm *(Wu, 2022)*, meeting the design requirements. By substituting the above parameters into Equation (1), the centroid-distance between the straight rod and the curved bar on the Y-axis (L_h) can be calculated from the gap between the curved rod and the curved bar (L_l) as Equation (2).

$$L_h = \sqrt{1296 - \left(L_l + 10\right)^2} \tag{2}$$

Equation (2) reveals a gradual decrease in L_h as L_l increases. The center of mass spacing (L_h) between the straight bar and the curved bar on the Y-axis is one of the crucial parameters to stop the sweet potato from rolling downward after popping up. A too-small L_h parameter increases the risk that the sweet potato will cross the straight bar. This study chose a gap of 20 mm between the curved bars (L_l) to increase both L_h and L_l to larger values. The calculation of Equation (2) approximates L_h to 20 mm, resulting in a center-of-mass spacing of 30 mm between the curved bars and the X-axis (L_s), which meets the design requirements.

Two-segment double buffer cleaning platform front drop buffer device design

During the sweet potato harvesting, the sweet potato falls from the elevator chain to the secondary double buffer cleaning platform. It then falls from the potato drop channel to the collection basket. These two stages are likely to cause sweet potato skin breakage. The double buffer cleaning platform incorporates a front falling buffer device and a rear conveying buffer device to decrease the rate of broken skin resulting from the falling and collision of sweet potatoes. The double buffer design effectively slows down the impact force of sweet potatoes during the falling process, thereby greatly reducing their damage. Figure 5 illustrates the structural design of the secondary double buffer cleaning platform device.

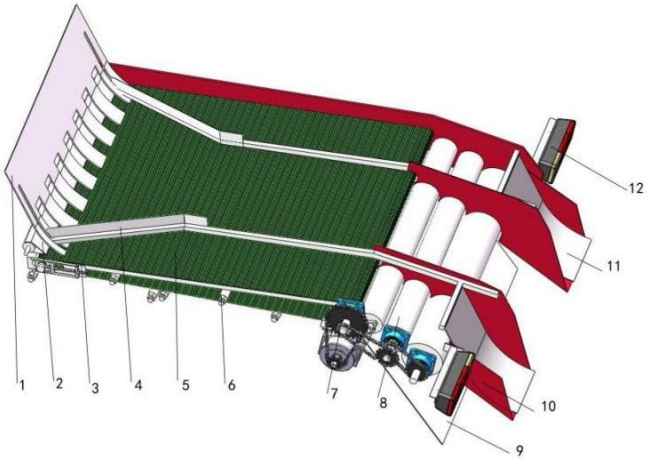

Fig. 5 - Structure of a Secondary Double Buffer Clearing Platform Device

1 - front rubber buffer curtain; 2 - front buffer protection plate; 3 - conveyor belt tensioning device; 4 - potato collection plate; 5 - clearing platform conveyor belt; 6 - rack support shaft; 7 - gear set; 8 - rear conveyor roller; 9 - sand leakage board; 10 - falling potato channel; 11 - rear rubber buffer curtain; 12 - tail light

The elevator chain's instantaneous throwing speed causes the sweet potato to continue moving in a vertical direction. This situation leads to a significant increase in the sweet potato's fall speed as well as a significant increase in the rate of broken skin. Therefore, the elevator chain ends with the installation of the front fall buffer device, which consists of a front rubber buffer curtain and a front buffer protection plate at the bottom of the conveyor belt. It can reduce the speed of sweet potato throwing and, at the same time, block the gravel and sand brought by the elevator chain to protect the pickers. Figure 6 shows that the sweet potato from the elevator chain falls to the secondary double buffer cleaning platform movement process, this time ignoring the potato-soil collision impact.

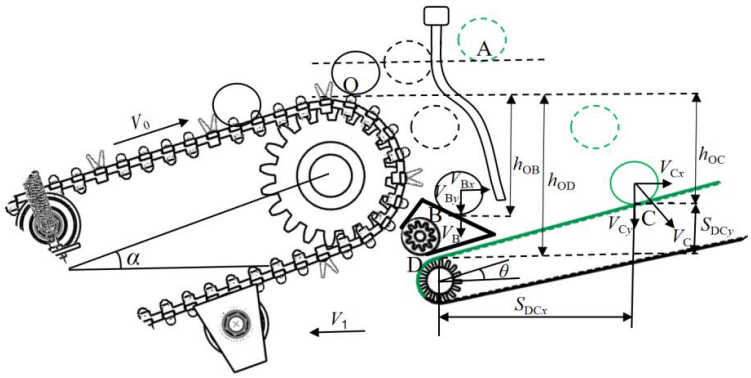

Fig. 6 - The movement of sweet potato falling from the elevator chain to the secondary double buffer cleaning platform

The conveyor belt on the cleaning platform is the reference surface for the sweet potato's displacement. Since the sweet potato and the conveyor belt are subject to the action of the vehicle speed V_1 simultaneously, the influence of the vehicle speed V_1 on the displacement of the sweet potato at this stage is negligible. This study viewed the OC section's motion without a front drop buffer device as the parabolic motion of a sweet potato, and by analyzing the kinematics of the sweet potato, the following formula was derived:

$$\begin{cases} V_C^{\,2} - V_0^{\,2} = 2gh_{OC} \\ h_{OC} = h_{OD} - S_{DCx}\tan\theta \\ S_{DCx} = V_{Cx}t_{OC} - V_{Bx}t_{OB} \\ V_{Cx} = V_0\cos\alpha \\ V_C = -V_0 + gt_{OC} \end{cases} \quad (3)$$

where:

V_C is the combined speed of sweet potatoes falling in the OC section, [m/s]; V_0 is the speed of the "d" type elevator chain, [m/s]; g is the acceleration of gravity, [m/s²], and g is valued at 9.8. h_{OC} is the vertical distance from point O to point C, [m]; h_{OD} is the vertical distance from point O to point D, [m]; S_{DCx} is the horizontal distance from point D to point C, [m]; θ is the inclination angle of the conveyor belt, [°]; V_{Cx} is the horizontal component velocity at the moment of falling of the sweet potato in the OC section, [m/s]; t_{OC} is the time of the sweet potato's movement from point O to point C, [s]; V_{Bx} is the horizontal component velocity at the moment of falling of the sweet potato in the OB section, [m/s]; t_{OB} is the time of the sweet potato's movement from point O to point B, [s]; α is the angle of the elevator chain and the ground, [°].

When the sweet potato is thrown up, due to the role of the front rubber buffer curtain, the speed of the sweet potato in the x-direction is gradually reduced to 0, so there is no speed effect on the sweet potato in the y-direction. Therefore, the velocity analysis in the y direction for the OB section of the front drop buffer device can be considered a free-fall motion, yielding the following formula:

$$\begin{cases} V_{Bx} = 0 \\ V_B^{\,2} = V_{By}^{\,2} = 2gh_{OB} \end{cases} \quad (4)$$

In the OB and OC sections, the sweet potato movement process follows the law of energy conservation. Therefore, this study analyzes the scenario with and without the shelter curtain and discovers that the sweet potato generates energy change before coming into contact with the conveyor belt.

$$\Delta E = \Delta E_{OB} - \Delta E_{OC} = \frac{1}{2} m V_B{}^2 - \frac{1}{2} m V_C{}^2 \tag{5}$$

Substituting Equation (3) and Equation (4) into Equation (5), the simplification leads to the following:

$$\Delta E = \frac{m}{2}\left[2gh_{OB} - V_0{}^2 - 2gh_{OD} + 2\left(V_C + V_0\right)V_0 \cos\alpha \tan\theta\right] \tag{6}$$

Among them, the static friction coefficient between sweet potato and nitrile rubber (NBR) is μ=0.61, and the friction coefficient between sand and rubber takes a value ranging from 0.605 to 0.621 (*Shen, 2021;* Yang *et al., 2021*). To ensure that the sweet potato and sandy soil are steadily elevated on the conveying rubber belt, the inclination angle θ of the sweet potato on the rubber belt should satisfy $\theta \leq \arctan 0.605$, that is, $\theta \leq 31.17°$. In conjunction with the pickup personnel at work on the pickup height, the conveyor belt inclination angle was set to 18°. Figure 5 illustrates that after designing the transmission ratio for each gear diameter, the h_{OD} approximation takes the value of 35 cm, and the h_{OB} approximation takes the value of 30 cm. It can be seen from Equation (6) that the speed of the elevator chain and the inclination angle of the elevator chain are within the range of meeting agronomic demand, and the energy change is maintained at $\Delta E<0$. It indicates that the installation of buffer curtains and buffer protection boards can effectively reduce the initial energy of the instant sweet potato falling, thereby reducing the rate of broken skin on the sweet potato. In summary, this study determined that the buffer protection plate's sloping surface had an inclination angle of 45° and a width of 7 cm, meeting the design requirements.

Two-segment double buffer cleaning platform rear conveyor buffer device design

The cleaning platform's conveyor belt transports the clean sweet potatoes to the rear conveying roller. At this time, the sweet potatoes have a faster final velocity and a higher falling height, which makes it easy to cause them to break their skin. Therefore, this study installs a rear conveyor buffer device at the end of the cleaning platform's conveyor belt, which directs the sweet potatoes into the potato collection channel through the rear conveyor roller. It also installs a rear rubber buffer curtain on the potato collection channel's surface to ensure stable transportation. To ensure stable transportation of the sweet potatoes on the rear conveying roller, the force analysis in Figure 7 illustrates the relationship between the sweet potatoes and the roller.

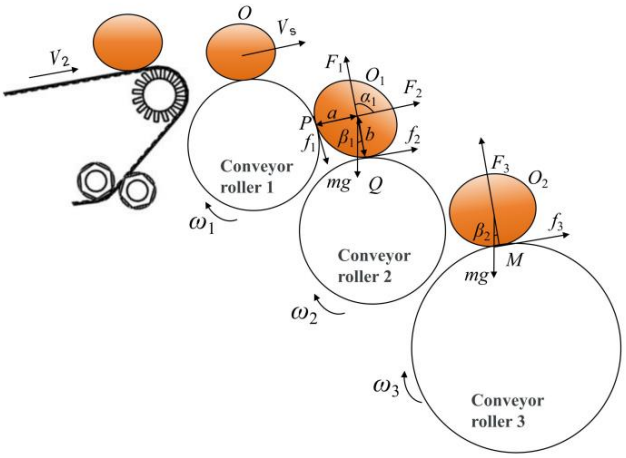

Fig. 7 - Force analysis of sweet potato between rear conveyor rollers of a secondary cleaning platform

O denotes that the sweet potato is transported in the conveying roller 1, and O_1 denotes the force analysis of the sweet potato under the simultaneous action of the two conveying rollers. When the sweet potato generates motion under the action of conveying rollers, it should satisfy that the resultant moment and resultant force at point Q are more than zero. O_2 denotes the force analysis performed by a single conveying roller.

$$\begin{cases} \sum\limits_{Q} M = \mu F_2 \left[a + b\sin\left(\alpha_1 - \dfrac{\pi}{2}\right)\right] + mgb\sin\beta_1 - F_2 b\sin\left(\pi - \alpha_1\right) \geq 0 \\ \sum\limits_{Q} F = \mu F_2 \cos\alpha_1 - mgb\sin\beta_1 + \mu F_1 + F_2\cos\left(\pi - \alpha_1\right) \geq 0 \\ \sum\limits_{M} F = mg\sin\beta_2 - \mu F_3 \end{cases} \tag{7}$$

where:

μ is the friction coefficient of sweet potato on the conveying roller; a is the distance between the center of mass of O_1 and the point P, [mm]; b is the distance between the center of mass of O_1 and the point Q, [mm]; α_1 is the angle between the support force F_1 and F_2, [°]; mg is the gravity of O_1, [N]; β_1 is the angle between the gravity of the sweet potato and the distance b, [°]; F_2 is the support force of sweet potato at the point P, [N]; β_2 is the angle between the gravity of the sweet potato and the O_2M, [°], and the O_2M is the line connecting the center of mass of O_2 to the contact point M.

The analysis of sweet potato force revealed that the sweet potato's gravity, which is impossible to regulate artificially, primarily affects the support force and friction force in Equation (7). However, it can affect the values of α_1, β_1, and β_2 by changing the dimensions and position of the rear conveying roller and making the sweet potato transport stable. Figure 6 and Equation (7) show that increasing the diameter of conveying roller 2 leads to an increase in α_1. It increases the resultant moment and resultant external force at the Q point, thereby enhancing the power of the sweet potato's tumble. Increasing the diameter of conveying roller 3 increases β_2, that is, increasing the resistance of the sweet potato at point M diagonally downward. Meanwhile, this causes an increase in the transportation distance on the conveying roller's surface, which can effectively reduce the sweet potato's transportation speed. As a result, it is necessary to reduce the transportation speed of the sweet potatoes to ensure that they have enough power to turn over each conveying roller. The size of the rear conveying roller can be set to gradually increase, which is conducive to the stable transportation of sweet potatoes. Combining the structural design of the secondary cleaning platform, which determines that the diameter of conveying roller 1 is 8 cm and the diameter of conveying roller 2 is 10 cm, ensures the stable transportation of sweet potatoes. Determine that the diameter of conveying roller 3 is 18 cm, aiming to guarantee the transportation of sweet potatoes while at the same time reducing its transportation speed. Wrapping NBR on the conveying roller's surface results in a static friction coefficient of μ=0.61, which improves conveying performance.

Key experimental parameters - Vibration frequency

In the sweet potato harvesting process, in order to prevent the sweet potato from crossing the straight bar strip from appearing to be repeatedly falling and thus causing damage, the amplitude and frequency of the vibration axis need to be limited. As shown in Figure 8, sweet potatoes with different short-axis radii have a high probability of being in the curved bar interval when stabilized *(Yang R.B. et al., 2024)*. The minimum force required for the sweet potato to cross the straight bar is the critical velocity V_t required for the movement of B to C.

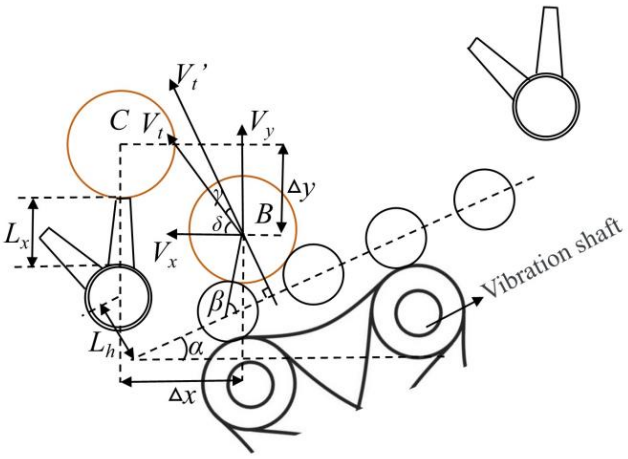

Fig. 8 - Motion analysis of sweet potato as it passes through the vibrating device during the lift-off process

The horizontal displacement Δx and vertical displacement Δy required for the sweet potato to move from B to C in the critical state are as follows:

$$\begin{cases} \Delta x = \left(L_h \tan\alpha + L_s\right)\cos\alpha + \dfrac{1}{2}\left(d_g + d_s\right)\cos\left(\beta + \alpha\right) \\ \Delta y = L_h \cos\alpha - L_s \sin\alpha + d_x + L_x + \dfrac{1}{2}\left(d_g + d_s\right)\left[1 - \sin\left(\beta + \alpha\right)\right] \end{cases} \quad (8)$$

where:

Δx is the horizontal displacement of the sweet potato, [mm]; Δy is the vertical displacement of the sweet potato, [mm]; and L_x is the height of the rubber sleeve of the straight bar, which is approximated as the distance between the sweet potato and the rubber sleeve of the outer ring of the straight bar in the critical state in the collision analysis, [mm]. β is the angle of the sweet potato B when it is stationary at the interval of the bent bar [°]. Analyzed from Figure 8, $cos\beta = L_s / \left(d_s + d_g\right)$.

According to the equations for uniformly decelerated linear motion in the vertical state and uniformly accelerated linear motion in the horizontal state, the critical velocity V_t required for the sweet potato to move from B to C is:

$$V_t = \sqrt{V_x^{\,2} + V_y^{\,2}} = \sqrt{\frac{g\Delta x^2}{2\Delta y} + 2g\Delta y} \tag{9}$$

where:

V_y is the component velocity of sweet potato in the vertical direction, [mm/s]; V_x is the component velocity of sweet potato in the horizontal direction, [mm/s]; g is the acceleration of gravity, [m/s^2], and g takes the value of 9.8.

The critical velocity, V_t, is at an angle δ in the horizontal direction:

$$\delta = arc\tan\frac{V_y}{V_x} = arc\tan\frac{2\Delta y}{\Delta x} \tag{10}$$

The elevator chain, with the vibration axis rotating to periodic up-and-down reciprocating motion, can be regarded as "simple harmonic motion", as shown in Figure 8 *(Lv et al., 2017)*. Set the vibration device to start at $t=0$, and the elevator chain's displacement in the vertical chain surface is 0. In one cycle, the vibration axis can provide four times the maximum amplitude. The elevator chain and the vibrating shaft share the same resonance frequency, allowing us to derive the following relationship between the vibration displacement Y and time t:

$$Y = \frac{A}{2}\cos\left(4\pi f \cdot t + \pi\right) + \frac{A}{2} \tag{11}$$

where:

Y represents the elevator chain's displacement on the vertical chain surface, [mm]; f signifies the vibration shaft's frequency, [Hz]; and A signifies the vibration shaft's maximum amplitude, [mm].

This study solves the derivative of Y with respect to t to derive the velocity V_t', which the vibrating device provides to the elevator chain perpendicular to the chain surface:

$$V_t^{'} = -2A\pi f \sin\left(4\pi f \cdot t + \pi\right) \tag{12}$$

To prevent the sweet potato from crossing the straight bar and causing repeated damage, the vibration device's maximum collision velocity, V_t', must ensure that the component velocity on the trajectory of the sweet potato from B to C is always smaller than the critical velocity, V_t. Figure 8 shows that V_t' takes the maximum value of $2A\pi f$, and there exists an angle γ between the maximum collision velocity Vt' and the critical velocity V_t, which yields the following equation.

$$2A\pi f \cos\left(\frac{\pi}{2} - \alpha - \arctan\frac{2\Delta y}{\Delta x}\right) < \sqrt{\frac{g\Delta x^2}{2\Delta y} + 2g\Delta y} \tag{13}$$

Combined with the above elevator chain structure design and actual operational requirements, the optimal amplitude A of the vibration shaft of the sweet potato combine harvester is 18.2 mm *(Liu, 2021)*. Equation (13) indicates that a sweet potato crossing the straight bar can cause repeated damage when f is less than 8.4. Simultaneously, if the vibration frequency is too low, it will result in a poor separation effect between the potato and soil, so the vibration shaft frequency f takes the value of 3-8 Hz.

Key experimental parameters - Elevator chain speed

Too slow a speed on the elevator chain is likely to cause congestion of the potato-soil mixture, and too fast a speed is likely to damage the sweet potato. To ensure stable transportation of the potato-soil mixture, the elevator chain's speed, and the harvester's forward speed should meet the following formula:

$$V_1 = \lambda V_0 \tag{14}$$

where:

V_1 is the forward speed of the harvester, [m/s]; λ is the speed coefficient, which generally takes the value of 0.8-2.5 *(Lv et al., 2015)*; and V_0 is the speed of the elevator chain, [m/s].

The faster the harvester advances, the greater the sweet potato harvest area per unit of time. However, too fast forward speed may lead to more impacts and friction on the sweet potato during digging and conveying, thus increasing its rate of broken skin. The sweet potato planting method involves planting two rows on one ridge, meaning that the agronomic characteristics of sweet potato planting and the picker's working speed influence the forward speed of the harvester.

$$V_1 = \frac{X \eta d}{2n} \tag{15}$$

where:

X is the number of pickers; η is the number of sweet potatoes picked up per second by a single picker; d is the distance between sweet potato plants, [m]; n is the number of sweet potatoes contained per plant.

During the sweet potato harvesting period, agronomic investigations and operational efficiency analyses were carried out. The harvester has four pickers and can pick 2-3 sweet potatoes per second. The sweet potato plant spacing is 0.3 m, and each plant bears 3-6 potatoes. Calculated by Equation (15), the forward speed of the harvester is in the range of 0.2-0.6 m/s. Usually, the ratio of the speed of the elevator chain to the speed of the vehicle during harvesting is slightly more than 1 *(Chen et al., 2019)*. So, in this paper, λ is taken to be 0.85. Equation (14) calculates the selected range of elevator chain speed V_0, which is 0.235-0.706 m/s. The elevator chain speed V_0 is 0.25-0.75 m/s for convenience of calculation.

Key experimental parameters - Clearing platform speed

Figure 7 demonstrates how the throwing velocity V_s of sweet potato O influences the sweet potato's falling position at the conveying roller. This indicates that it affects α_1, β_1, and β_2 in Equation (7), which affects the stability of sweet potato transportation. The V_s is affected by both the velocity V_2 of the clearing platform and the angular velocity ω_1 of the rearward conveyor roller 1. This study employs gears and chain connections to maintain consistency between the speed of the cleaning platform and the linear speed of the conveyor roller 1, thereby minimizing the risk of skin breakage of sweet potatoes that fall onto the conveyor roller 1 due to their significant speed differences. Therefore, cleaning platform speed V_2 is one of the key factors affecting sweet potato harvesting. Yang determined that the clearing platform of the secondary conveying and separating device has a speed range of 0.4-0.8 m/s *(Yang R.B. et al, 2024)*.

Key performance parameters - The rate of broken skin of sweet potatoes

In this field trial, the sweet potato skin-breaking rate (B_R) and impurity rate (I_R) were used as evaluation indices, referencing the DG/T078-2022 potato harvester operation standard in the "Agricultural Machinery Extension Appraisal Syllabus" *(Ministry of Agriculture and Rural Affairs, 2022)*. Equation (16) describes how to calculate the skin-breaking rate as follows:

$$B_R = \frac{m_3}{m_1 + m_2} \times 100\% \tag{16}$$

where:

B_R is the sweet potato skin-breaking rate, [%]; m_1 is the total mass of harvested sweet potato in two trips, [kg]; m_2 is the total mass of missed pickup sweet potato in two trips, [kg]; m_3 is the total mass of skin-breaking sweet potato, [kg].

Key performance parameters - Impurity rate of sweet potatoes

Determination of impurity content refers to the ratio of impurities in the potato box after harvest to the total mass of the box, which includes small potatoes, vines, and soil mass. The impurity rate was calculated according to Equation (17), which is described below:

$$I_R = \frac{m_4}{m_1 + m_4} \times 100\% \quad (17)$$

where: I_R is the impurity content of sweet potato, [%]; m_4 is the mass of impurities, [kg].

Method of field experiment

The field experiment site of this study was the sweet potato planting base of the Intelligent Agricultural Machinery (Nada Town, Danzhou City, Hainan Province, China). The sweet potato variety was “GaoXi 14”, the width of the sweet potato ridge was 650 mm, the width of the bottom of the ridge was 1000 mm, the height of the ridge was 200 mm, the soil compactness of the bottom of the ridge was 1305 kPa, the density of the soil was 1.82 g/cm^3, and the water content was 12.87 %. Instruments and equipment required for the test included a low-damage fresh-eating sweet potato combine harvester, a non-contact tachometer (DLY-2301), an electronic protractor (precision of 0.01), a potato collection basket, and an electronic scale.

To investigate the variation rule of vibrating shaft frequency, elevator chain speed, and clearing platform speed on the effect of skin-breaking rate and impurity rate, as well as to obtain the optimal parameter combination, this study combines the previous analysis to determine that the vibrating shaft frequency f is 3-8 Hz, the elevator chain speed V_0 is 0.25-0.75 m/s, and the cleaning platform speed V_2 is 0.25-0.75 m/s. The skin-breaking rate of sweet potatoes and the impurity rate were taken as the evaluation indexes. Table 2 displays the test factor level codes.

Table 2

Factor level coding table

Level	Experimental factor		
	A: Vibrating shaft frequency (Hz)	B: Elevator chain speed (m/s)	C: Cleaning platform speed (m/s)
-1	3	0.25	0.4
0	5.5	0.5	0.5
1	8	0.75	0.8

This study used Design-Expert 13.0 to conduct a three-factor, three-level Box-Behnken test, repeating each set of tests three times to get the average *(Ferreira et al., 2007; Chen et al., 2024)*. Table 3 displays the experimental results.

Table 3

Response surface results

Trial No.	Experimental Factors			Evaluation Indicator	
	A (Hz)	B (m/s)	C (m/s)	B_R (%)	I_R (%)
1	3	0.25	0.6	0.95	2.47
2	8	0.25	0.6	1.18	1.77
3	3	0.75	0.6	1.42	3
4	8	0.75	0.6	1.51	2.5
5	3	0.5	0.4	1.38	1.75
6	8	0.5	0.4	1.47	1.53
7	3	0.5	0.8	1.04	2.81
8	8	0.5	0.8	1.37	1.86
9	5.5	0.25	0.4	1.29	1.74
10	5.5	0.75	0.4	1.86	2.12
11	5.5	0.25	0.8	1.25	2.56
12	5.5	0.75	0.8	1.58	2.95
13	5.5	0.5	0.6	1.1	1.82
14	5.5	0.5	0.6	1.11	1.92
15	5.5	0.5	0.6	1.19	1.84
16	5.5	0.5	0.6	1.18	1.82
17	5.5	0.5	0.6	1.18	1.89

The field experiment and the effect are shown in Figure 9.

(a) (b)

Fig. 9 - Field experiment

RESULTS

Regression equation analysis of field experiment results

As shown in Table 4, the Design Expert 13 software fitted the data to determine the significance of each influential factor, and it performed an ANOVA for B_R and I_R to establish the regression equation.

Table 4

ANOVA for regression equations

	Broken skin B_R [%]					Impurity content I_R [%]				
Source	**Sum of Squares**	**D/F**	**Mean Square**	***F*-value**	***P*-value**	**Sum of Squares**	**D/F**	**Mean Square**	***F*-value**	***P*-value**
Model	0.8029	9	0.0892	53.01	< 0.0001**	3.52	9	0.3909	58.65	< 0.0001**
A-Vibration shaft frequency	0.0685	1	0.0685	40.67	0.0004**	0.7021	1	0.7021	105.34	< 0.0001**
B-Lift chain speed	0.3613	1	0.3613	214.66	< 0.0001**	0.5151	1	0.5151	77.29	< 0.0001**
C-Cleaning platform speed	0.0722	1	0.0722	42.90	0.0003**	1.16	1	1.16	173.32	< 0.0001**
AB	0.0049	1	0.0049	2.91	0.1317	0.0100	1	0.0100	1.50	0.2602
AC	0.0144	1	0.0144	8.56	0.0222*	0.1332	1	0.1332	19.99	0.0029**
BC	0.0144	1	0.0144	8.56	0.0222*	0.0000	1	0.0000	0.0038	0.9529
A²	0.0047	1	0.0047	2.81	0.1377	0.0519	1	0.0519	7.78	0.0269*
B²	0.0904	1	0.0904	53.70	0.0002**	0.9143	1	0.9143	137.19	< 0.0001**
C²	0.1626	1	0.1626	96.61	< 0.0001**	0.0014	1	0.0014	0.2162	0.6561
Residual	0.0118	7	0.0017			0.0467	7	0.0067		
Lack of Fit	0.0043	3	0.0014	0.7665	0.5694	0.0386	3	0.0129	6.37	0.0529
Pure Error	0.0075	4	0.0019			0.0081	4	0.0020		
Cor Total	0.8147	16				3.57	16			
R²	0.9855					0.9869				

Note: $P < 0.01$ indicates highly significant, **; $0.01 < P < 0.05$ indicates significant, *.

Table 4 reveals that the rates of broken skin and impurity rate regression models are highly significant, whereas the lack of fit relationship is not. It indicates that the regression model analysis can better reflect the relationship between the skin-breaking rate or impurity rate, the vibration shaft frequency, the elevator chain speed, and the cleaning platform speed. The factors A, B, C, AC, B^2, and C^2 have highly significant effects on B_R, whereas the factors AC and BC have significant effects on B_R. According to the F values of A, B, and C, the three factors have a significant impact on the skin-breaking rate in the order of elevator chain speed, cleaning platform speed, and vibrating shaft frequency. The factors A, B, C, AC, and B^2 have a highly significant impact on I_R, while A^2 significantly influences I_R in the order of clearing platform speed, vibrating shaft frequency, and elevator chain speed.

The non-significant terms are not involved in the data analysis, so the regression model of B_R and I_R is optimized as follows:

$$\begin{cases} B_R = 3.162 - 0.035A - 0.746B - 6.377C + 0.12AC - 1.2BC + 2.316B^2 + 4.868C^2 \\ I_R = 2.075 - 0.097A - 6.457B + 3.908C - 0.365AC + 0.018A^2 + 7.472B^2 \end{cases} \quad (18)$$

After optimizing the regression model, the coefficient of determination R^2 for B_R is 0.9737, meaning it can explain approximately 97.37% of the variation in the response variable. The coefficient of determination R^2 of I_R is 0.9837, which indicates that the regression model about I_R can explain about 98.37% of the variation in the response variable. The closeness of the R^2 to 1 signifies that a better fit of the model results in a smaller difference between the predicted and actual values. To show more intuitively the fitting degree of the optimized regression model, the predicted and actual values are plotted as line graphs for analysis. Figure 10(a) shows the comparison results between the actual and predicted values of B_R, and Figure 10(b) demonstrates the comparison results between the actual and predicted values of I_R. In this case, green line segments represent the actual values, while red lines represent the predicted values. The figure clearly shows a satisfactory fit between the predicted and actual values.

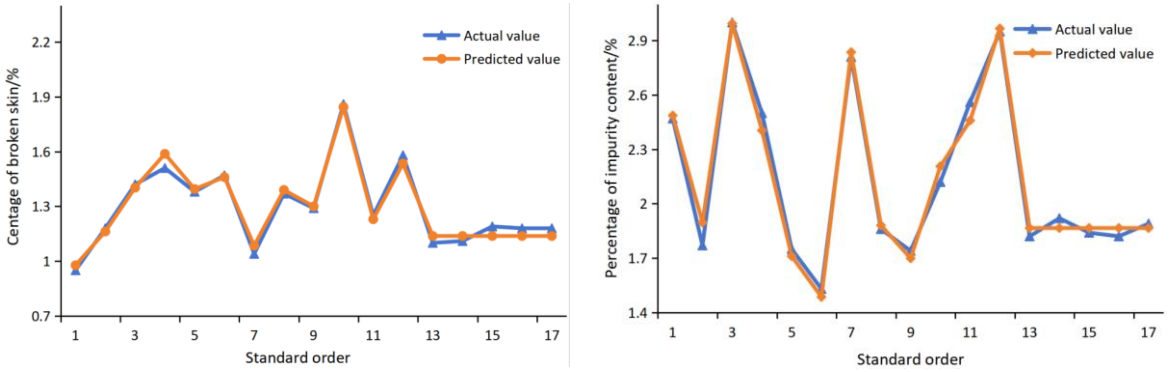

(a) *(b)*

Fig. 10 - Comparison of data predicted by regression models

(a) Comparison of data predicted by B_R regression models; (b) Comparison of data predicted by I_R regression models

Parameter Optimization

The quality and integrity of sweet potatoes are key factors affecting their marketing. The sweet potato's B_R significantly influences its quality, with a set weight of 70%. In contrast, I_R primarily influences the efficiency of sweet potato harvesting and has a relatively small impact on sweet potato quality, with a set weight of 30%. To further investigate the optimal parameters of the harvesting process, it is necessary to perform parameter optimization on the above experimental results and construct a mathematical model. The optimized objective function and determined constraints are as follows:

$$\begin{cases} minB_R(A,B,C) \\ minI_R(A,B,C) \\ s.t.\begin{cases} 3 \le A \le 8 \\ 0.25 \le B \le 0.75 \\ 0.4 \le C \le 0.8 \end{cases} \end{cases} \quad (19)$$

Parameter optimization determines the optimal combination of parameters. Among them, the vibrating shaft frequency was 5.153 Hz, the elevator chain speed was 0.368 m/s, and the clearing platform speed was 0.578 m/s. At this point, the B_R of sweet potatoes was 1.06%, and the I_R was 1.86%.

Field experiment validation

The field experiment was conducted using the best parameter combination to verify the accuracy of the above regression equation and the best parameter combination, and the results are shown in Figure 11. The B_R and I_R of sweet potatoes were analyzed under this parameter condition. This test was conducted at the Intelligent Agricultural Machinery and Equipment Research Institute's sweet potato planting base (Nada Town, Danzhou City, Hainan Province, China). After taking the approximate values, the experimental parameters yielded a vibrating shaft frequency of 5.2 Hz, an elevator chain speed of 0.37 m/s, and a clearing platform speed of 0.58 m/s. Table 4 displays the experimental results, revealing a B_R of 1.09 % and an I_R of 1.90 % for sweet potatoes. Despite the slight increase in B_R and I_R, the relative errors were less than 5 %, indicating the reliability of the regression model.

Fig. 11 - Field experiment to verify harvesting effectiveness

Table 5

Experimental validation results

Items	B_R	I_R
Predicted Value	1.06%	1.86%
Validation Value	1.09%	1.90%
Relative Error	2.83%	2.15%

Discussion

This research processed the data from Table 4 and combined it with the response surface results to analyze and explain the test factors that significantly affected B_R and I_R.

Table 4 reveals that the vibration shaft frequency and the cleaning platform speed significantly influence B_R, with Figure 12(a) displaying the response surface. Meanwhile, the elevator chain speed is 0.5 m/s, and the B_R increases gradually as the vibrating shaft frequency. This indicates that the higher frequency of the vibration axis makes the number of collisions between sweet potatoes and bars increase. This situation makes it easy for the sweet potatoes to cross the straight bars, resulting in repeated falls and collisions that increase B_R.

Figure 12(a) shows that B_R tends to decrease and then increase as the cleaning platform's speed increases. It indicates that when the speed of the clearing platform is small, the number of sweet potatoes piled up on the clearing platform per unit time is larger. Meanwhile, the slow speed of the rear conveyor roller may lead to the accumulation and jamming of sweet potatoes, and the friction between sweet potatoes increases the B_R. If the clearing platform's speed is excessively high, it could potentially damage the sweet potatoes during the conveying process due to the high impact force, thereby increasing the B_R.

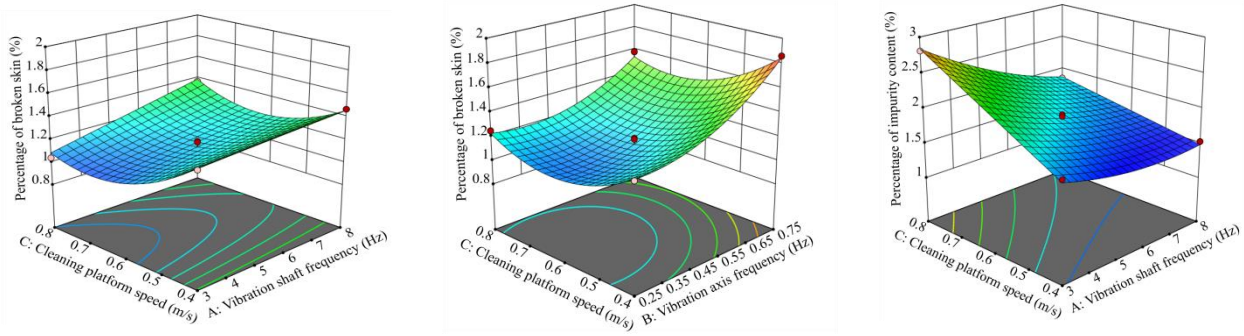

(a) *(b)* *(c)*

Fig. 12 - Significant and highly significant interaction response surfaces

(a) AC interaction response surface of B_R; (b) BC interaction response surface of B_R; (c) AC interaction response surface of I_R

Table 4 shows that elevator chain speed and clearing platform speed have a significant influence on B_R. Figure 12(b) displays the response surface, where the vibration axis frequency is 5.5 Hz. Figure 12(b) shows that the B_R increases gradually as the elevator chain speed increases.

When the elevator chain speed is low, the number of collisions between the sweet potato and the elevator chain bars is smaller, and the collision amplitude is small. As a result, the B_R remains at a low level with no obvious changes. As the elevator chain speed increases, the sweet potato generates more friction as it passes through the vibrating shaft and the rollers, leading to a significant increase in B_R and more noticeable changes.

Table 4 demonstrates that the vibration shaft frequency and the clearing platform's speed significantly influence the I_R, as depicted in Figure 12 (c), where the elevator chain's speed is 0.5 m/s. Figure 12 (c) shows that the I_R decreases gradually as the vibration shaft frequency increases. It shows that increasing the vibration shaft frequency will make the number of collisions between the impurities increase, which leads to the impurities gradually falling into the ground from the bar gap, reducing the I_R.

Figure 12(c) shows that I_R increases gradually as the clearing platform speeds up. It indicates that when the speed of the cleaning platform is less, the soil attached to the sweet potato can be cleaned out by the rear conveyor roller, and the broken soil removed is discharged to the surface through the sand leakage plate, which reduces the I_R of the sweet potato. The cleaning platform's increased speed prevents the timely completion of manual and conveyor roller cleaning operations, resulting in a gradual increase in I_R.

CONCLUSIONS

(1) This study designed a low-damage fresh-eating sweet potato combine harvester based on a two-segment potato-soil separating device and described its whole machine structure and working principle. The one-segment potato-soil separator device is designed with a “d” type elevator chain structure and a vibrating device. The two-segment double buffer cleaning device incorporates a front-falling buffer device and a rear-conveying buffer device. This harvester can effectively solve the problem of high B_R and I_R in the sweet potato harvesting process.

(2) The paper presents a design that uses a straight bar on the elevator chain and a kinematic analysis of sweet potatoes to prevent falls. The study shows that using a vibration axis frequency (*f*) of 3-8 Hz can reduce collisions and mitigate repeated damage caused by sweet potatoes hitting the straight bar. This research determined the speed of the elevator chain V_0 as 0.25-0.75 m/s through the agronomic survey of sweet potato planting and the analysis of pickers' operating efficiency. The analysis of the sweet potato force in the rear conveyor roller of the secondary cleaning platform determines the speed of the cleaning platform V_2 to be 0.4-0.8 m/s.

(3) This research conducted the quadratic regression orthogonal combination test, using the vibrating shaft frequency, elevator chain speed, and cleaning platform speed as test factors and the B_R and I_R as evaluation indexes. The results indicate that reducing the vibration shaft frequency and elevator chain speed and increasing the cleaning platform speed appropriately can reduce the B_R of the sweet potato harvesting process. Conversely, increasing the vibration shaft frequency and elevator chain speed appropriately and decreasing the cleaning platform speed can reduce the I_R of the sweet potato harvesting process. The field validation results showed that the optimal parameter combinations were a vibrating shaft frequency of 5.2 Hz, an elevator chain speed of 0.37 m/s, and a cleaning platform speed of 0.58 m/s.

At this time, the B_R of sweet potatoes was only 1.09 %, and the I_R was only 1.90 %, which meets the design standard of potato harvesting machinery. Overall, this harvester can significantly improve harvesting efficiency, and there is an obvious improvement in sweet potato B_R and I_R.

ACKNOWLEDGEMENT

Research on the device and mechanism of low damage cassava coupled excavation based on dynamic rupture characteristics of cassava-soil complex. (Project No. 52265029).

REFERENCES

[1] Beznosyuk R.V., Evtekhov D.V., Borychev S.N., Kostenko M.Y., Rembalovich G.K., (2022), Justification of parameters of a finger hump of potato harvesters when vibrating canvas, *IOP Conference Series: Earth and Environmental Science*, vol. 981, no. 4, ISSN 1755-1315, p. 042051, United Kingdom.

[2] Bovell-Benjamin A.C., (2007), Sweet Potato: A Review of its Past, Present, and Future Role in Human Nutrition, *Advances in Food and Nutrition Research*, vol. 52, ISSN 1043-4526, pp. 1–59, Valencia/Spain.

[3] Bulgakov V., Bonchik V., Holovach I., Fedosiy I., Volskiy V., Melnik V., Ihnatiev Ye., Olt J., (2021), Justification of parameters for novel rotary potato harvesting machine, *Agronomy Research*, vol. 19, no.2, ISSN 1406-894X, pp. 1–11, Estonia.

[4] Chen M., Liu X., Hu P., Zhai X., Han Z., Shi Y., Zhu W., Wang D., He X., Shang S., (2024), Study on rotor vibration potato-soil separation device for potato harvester using DEM-MBD coupling simulation, *Computers and Electronics in Agriculture*, vol. 218, ISSN 0168-1699, p. 108638, United Kingdom.

[5] Chen X.D., Hu Z.C., Wang B., You Z.Y., Peng B.L., Hu L.L., (2019), Design and parameter optimization of sweet-potato-stalk separator for single row sweet potato combine harvester (单垄单行甘薯联合收获机薯秧分离机构设计与参数优化), *Transactions of the Chinese Society of Agricultural Engineering (Transactions of the CSAE)*, vol. 35, no. 14, ISSN 1002-6819, pp. 12-21, Beijing/China.

[6] Chen X.D., (2020), *Study Sweet-potato-stalk Separation Characteristics and Structure Optimization of in Self-propelled Sweet Potato Combine Harvester (自走式甘薯联合收获机薯茎分离特性研究与机构优化)*, Master's Thesis, Anhui Agriculture University, Anhui/China.

[7] Cláudio E. Cartabiano-Leite, Ornella M. Porcu, Alicia F. de Casas, (2020), Sweet potato (Ipomoea batatas L. Lam) nutritional potential and social relevance: a review, *International Journal of Engineering Research and Applications*, vol. 10, no. 6, ISSN 2248-9622, pp. 23–40, India.

[8] Cui Z.K., Zhang H., Zhou J., Li T., (2020), Design and test of 4U-750 trailing type sweet potato harvester (4U-750 牵引式甘薯收获机设计与试验), *Journal of Chinese Agricultural Mechanization*, vol. 41, no. 5, ISSN 2095-5553, pp. 01-05, Jinan/China.

[9] dos Santos T.P.R., Franco C.M.L., Mischan M.M., Leonel M., (2019), Behavior of Sweet Potato Starch After Spray‐Drying Under Different Pretreatment Conditions, *Starch - Stärke*, vol. 71, no. 9–10, ISSN 0038-9056, 1521-379X, p. 1800245, Germany.

[10] Feng B., Wang H.C., Wang G.P., Sun W., Shi L.R., Tian B., (2024), Optimization and Experiment of Operating Parameters of Separating Screen of Small Potato Harvester (小型马铃薯收获机分离筛作业参数优化与试验), *Journal of Agricultural Mechanization Research*, vol.46, no.10, pp.138-144+152, Harbin/China.

[11] Ferreira S.L.C., Bruns R.E., Ferreira H.S., Matos G.D., David J.M., Brandão G.C., da Silva E.G., Portugal L.A., dos Reis P.S., Souza A.S., dos Santos W.N., (2007), Box-Behnken design: An alternative for the optimization of analytical methods, *Analytica Chimica Acta*, vol. 597, no.2, pp. 179–186, Netherlands.

[12] Hu L.L., Tian L.J., Ji F.L., Wang B., (2014), Research on the working mode of sweet potato production mechanization (甘薯生产机械化作业模式研究), *Journal of Chinese Agricultural Mechanization*, vol. 35, no. 5, ISSN 2095-5553, pp. 165-168, Nanjing/China.

[13] Fu Y., Ren S.Y., Tang P., Leng Y.C., Chen X.H., Tu X.Y., Lv X.R., (2023), Design and simulation test of digging device for small potato harvester, *INMATEH – Agricultural Engineering,* vol. 69, no. 1, ISSN 2068–4215, pp. 145-158, Romania.

[14] Hrushetsky S.M., Yaropud V.M., Duganets V.I., Duganets V.I., Pryshliak V.M., Kurylo V.L., (2019), Research of constructive and regulatory parameters of the assembly working parts for potato harvesting machines, *INMATEH – Agricultural Engineering*, vol. 59, no. 3, ISSN 2068–4215, pp. 101-110, Romania.

[15] Ismail Z.E., Amine E.E., El-Shabrawy T.H., Faleih H.S., (2014), Investigate a simple design for sweet potato harvesting, *Misr Journal of Agricultural Engineering*, vol. 31, no. 4, pp.1331–1346, Egypt.

[16] Liu C.L., (2021), *Study on Design and Damage Law of Sweet Potato Combine Harvester (甘薯联合收获输送分离装置设计及损伤规律研究)*, Master's Thesis, Shandong Agricultural University, Tai'an/China.

[17] Li J.C., Lv Y.N., Sun Y.K., Lin Y.L., (2022), Design and Experiment of Separating and Lifting Device of Potato Harvester-Based on Equivalent Radius Method (马铃薯收获机分离升运装置设计与试验——基于当量半径法), *Journal of Agricultural Mechanization Research*, vol. 44, no. 12, ISSN 1003-188X, pp. 199-206+256, Harbin/China.

[18] Li X.Q., Wang X.H., Liu Y., Wang F., Meng P.X., Wang J.M., (2023), Design and Experiment of Circular Reducing and Collecting Potato Lifting Device for Potato Combine Harvester (马铃薯联合收获机环形减损集薯升运装置设计与试验), *Transactions of the Chinese Society for Agricultural Machinery*, vol. 54, no. 12, ISSN 1000-1298, pp. 109-120, Beijing/China.

[19] Lv J.Q., Sun H., Dui H., Peng M.M., Yu J.Y., (2017), Design and Experiment on Conveyor Separation Device of Potato Digger under Heavy Soil Condition (粘重土壤下马铃薯挖掘机分离输送装置改进设计与试验), *Transactions of the Chinese Society for Agricultural Machinery*, vol. 48, no. 11, ISSN 1000-1298, pp. 146-155, Beijing/China.

[20] Lv J.Q., Tian Z.G., Yang Y., Shang Q.Q., Wu J.E., (2015), Design and experimental analysis of 4U2A type double-row potato digger (4U2A 型双行马铃薯挖掘机的设计与试验), *Transactions of the Chinese Society of Agricultural Engineering (Transactions of the CSAE)*, vol. 31, no. 6, ISSN 1002-6819, pp. 17-24, Beijing/China.

[21] Marciniak A., Przybyl K., Koszela K., Duda A., Szychta M., (2022), Analysis of the strength of an innovative design of an organic farming potato harvester, *In Journal of Physics: Conference Serie*s, vol. 2212, no. 1, ISSN 1742-6596, p. 012028, United Kingdom.

[22] Ministry of Agriculture and Rural Affairs, PRC, (2022), *Agricultural machinery promotion appraisal outline: potato harvester (农业机械推广鉴定大纲: 薯类收获机)*, DG/T 078-2022, 22.2.2022, Beijing/China.

[23] Mohanraj R., Sivasankar S., (2014), Sweet potato (Ipomoea batatas [L.] Lam)-A valuable medicinal food: A review. *Journal of medicinal food*, vol. 17, no. 7, ISSN 1096-620X, pp. 733-741, United States.

[24] Shen H.Y., (2021), *Sweet potato combined harvesting arc grid handover Research and Optimization of Scraper Chain Conveying Mechanism (甘薯联合收获弧栅交接刮板链输送机构研究与优)*, Master's Thesis, Chinese Academy of Agricultural Sciences Thesis, Nanjing/China.

[25] Wang B., Hu L.L., Hu Z.H., Tian L.J., Ji F.L., Ma B., (2014), Damage mechanism study of chain-lever elevator sweet potato harvester (链杆式升运器薯土分离损伤机理研究), *Journal of China Agricultural University*, vol. 19, no. 02, ISSN 1007-4333, pp. 174-180, Beijing/China.

[26] Wang F.A., Cao Q.Z., Li Y.B., Pang Y.L., Xie K.T., Zhang Z.G., (2023), Design and Trafficability Experiment of Self-propelled Potato Harvester in Hilly and Mountainous Areas (丘陵山区自走式马铃薯联合收获机设计与通过性试验), *Transactions of the Chinese Society for Agricultural Machinery*, vol. 54, no. s2, ISSN 1000-1298, pp. 10-19, Beijing/China.

[27] Wei Z.C, Han M., Su G.L., Zhang H., Li X.Q., Jin C.Q., (2023), Design and Experiment of a Bagging and Unloading Potato Combine Harvester (装包卸包型马铃薯联合收获机设计与试验), *Transactions of the Chinese Society for Agricultural Machinery*, vol. 54, no. 10, ISSN 1000-1298, pp. 92-104, Beijing/China.

[28] Wu D.Y., (2022), *Experimental Study on Collision Damage of Rod Lifting Chain to Potato and Parameter Design (马铃薯与杆条升运链碰撞损伤试验研究与参数设计)*, Master's Thesis, Northwest A&F University, Xianyang/China.

[29] Xie Y.Z., Bian X.F., Jia Z.D., Ma P.Y., Yu Y., Zhang Q., Liu S., (2022), Development status and prospect of fresh sweet potato industry in China (中国鲜食甘薯产业发展现状及其发展前景). *Jiangsu Journal of Agricultural Sciences*, vol. 38, no. 06, ISSN 1000-4440, pp. 1694-1701, Nanjing/China.

[30] Yang R.B., Zhang J., Shang S.Q., Tian G.B., Zhai Y.M., Pan Z.G., (2024), Design and Test of Secondary Conveyor Separator Device for Sweet Potato Combine Harvester (甘薯联合收获机二级输送分离装置的设计与试验), *Journal of Jilin University (Engineering and Technology Edition)*, ISSN 1671-5497, pp.1-14, Changchun/China.

[31] Yang S., Zheng M.J., Wu W.J., Zhao C.L., (2021), Calibration of Physical Characteristics of Wind Sand Particles Based on Discrete Element Method (基于离散元的风沙沙粒物理特性参数标定), *Journal of Shijiazhuang Tiedao University (Natural Science Edition)*, vol. 34, no. 01, ISSN 2095-0373, pp. 49-57. Shijiazhuang/China.

[32] Yang X., Wu Y., Wang L., Liu F., Zhao X., Bai H., Dong W., Kong X., Hu H., Zhong W., Xuan D., Yang A., Ma Y., (2024), Design and Performance Test of 4UJ-180A Potato Picking and Bagging Machine, *Agriculture*, vol. 14, no. 3, ISSN 2077-0472, p. 454, Basel/Switzerland.